Mater. Res. Soc. Symp. Proc. Vol. 1124 © 2009 Materials Research Society 1124-Q07-10

Evolution of the Geochemical Conditions in the Bentonite Barrier and its Influence on the Corrosion of the Carbon Steel Canister

Elena Torres [1], Alicia Escribano [1], Juan L. Baldonedo [2], María J. Turrero [1], Pedro L. Martín[1], Javier Peña [1], María V. Villar [1]
[1] Division of Engineered and Geological Barriers, CIEMAT, Avda. Complutense 22, 28040, Madrid, Spain.
[2] Centro de Microscopía Electrónica, Universidad Complutense de Madrid, Avda. Complutense s/n, 28040, Madrid, Spain

ABSTRACT

This work has been focused on characterization of geochemical processes occurring in the bentonite barrier and their influence on corrosion of the carbon steel container. In the cells used for these tests, a block of compacted bentonite was subjected simultaneously to constant hydration and heating, in opposite directions, in order to simulate the conditions of the clay barrier in the repository and better understand the coupled THMC (Thermo-Hydro-Mechanical-Chemical) processes that can affect the performance of the bentonite barrier or the metallic container. In these tests, carbon steel was substituted by Fe powder in order to enhance corrosion phenomena. At present, only two out of the six cells assembled have been dismantled after 6 and 15 months. In both cases, an advective movement of salts towards the heater has been observed. CEC values increased in saturated areas. In the exchange complex, Mg was replaced by Na in saturated areas, whereas in unsaturated zones close to the heater, Mg is the prevalent exchangeable cation. Goethite and hematite were the main corrosion products found in the 6-month and 15-month tests, respectively.

INTRODUCTION

Carbon steel is one of the candidate materials for the waste package in the Spanish High-Level Waste (HLW) Disposal Project. These waste packages will be emplaced in a granitic host formation. As buffer material, FEBEX bentonite (Na-Ca-Mg bentonite) has been chosen by the Spanish radioactive waste management agency as the reference bentonite.

The behavior of a HLW repository is determined by the characteristics of design of the engineered barrier system. The combined effect of the heat generated by radioactive decay and the ingress of groundwater can provoke changes in the mechanical, hydraulic and geochemical properties of the bentonite barrier. Geochemical conditions in the bentonite barrier surrounding the carbon steel container can compromise canister performance.

Chloride and sulfate move by advective transport towards the metallic container due to the constant hydration and heating of the clay barrier. Both chlorides and sulfates are hygroscopic salts. They are known to enhance corrosion of mild steel at relative humidity (RH) below 100% [1]. The aqueous salt films formed on the steel surface allow electrochemical corrosion to occur. Bulk aqueous solutions will form at values equal or greater than the equilibrium RH of the saturated salt solution. However, at RH values below the equilibrium

value there is an increase in the weight gain when compared to the corrosion in the absence of the deposited salt [2].

The aim of this work is, on one hand, to identify the different geochemical processes taking place in compacted bentonite as a function of the variations of the Thermo-Hydro-Mechanical (THM) parameters and, on the other hand, to characterize the corrosion products formed at an Fe/bentonite interface during the unsaturated state of bentonite.

EXPERIMENT

Materials

The experimental set-up consists on hermetic cells (figure 1a) where a compacted block of FEBEX bentonite (1.65 g/cm^3) in contact with Fe powder at its bottom is hydrated with reduced granitic water (Grimsel, Switzerland) (see table I) on the top while a thermal load is applied from the bottom. The body of the cell is made out of Teflon, although an external steel cylinder prevents its deformation by swelling. A plane heater (100ºC) constitutes the bottom of the cell while, on the top of the cell, a chamber allows the circulation of water at a controlled temperature (around 22ºC), so a thermal gradient is established. Two sensors, placed at 25 and 80 mm from the top of the bentonite block, record the evolution of RH and temperature as the hydration front advances.

Table I. Chemical composition of the granitic water used in the tests (Grimsel Test Site, Switzerland).

Chemical species	Na	Ca	Mg	K	SO_4^{2-}	Cl^-
Concentration (ppm)	15.0	5.9	<0.4	---	6.3	5.7
pH 9.72	**E_h** -200 mV			**Alk (HCO_3^-)**	23 ppm	

FEBEX bentonite is composed of 92±3% dioctahedral smectite of the montmorillonite type. It contains variable quantities of quartz (2±1%), plagioclase (2±1%), cristobalite (2±1%), potassium feldspar (traces), calcite (traces) and trydimite (traces). The cation exchange capacity is 102 meq/100g, and the exchangeable cations are Ca (35±3 meq/100g), Mg (31±3 meq/100g), Na (27.1±0.2 meq/100g) and K (2.6±0.4 meq/100g). The water content of the clay at laboratory conditions is about 13.7 ± 1.3 %.

Methods

To determine the exchangeable cations of the samples, a $CsNO_3$ solution was used to displace the exchangeable cations [3]. Soluble elements were analysed in aqueous extract solutions at a solid to liquid ratio of 1:8 (5 g of clay in 40 ml of deionized water reacted for 24 h.). Additional measures of soluble salts were realized at the interface. The sampling of the bentonite block is shown in figure 1b.

Iron powder was analysed by means of Transmission Mössbauer Spectroscopy (TMS), Scanning Electron Microscopy (SEM) coupled to Energy Dispersive X-ray Spectroscopy (EDS), Transmission Electron Microscopy (TEM) and Scattered Area Electron Diffraction (SAED).

RESULTS AND DISCUSSION

THM behavior

The distribution of water content along the bentonite columns in the tests occurs soon after the beginning of the experiment. As observed in figure 2, RH increases in the coldest end of the block, where hydration is applied. However, close to the Fe/bentonite interface, where temperature is about 100ºC, bentonite loses its absorbed water. Desiccation seems to take place rather quickly and affects especially the section closest to the heater, where RH values are lower than the initial values.

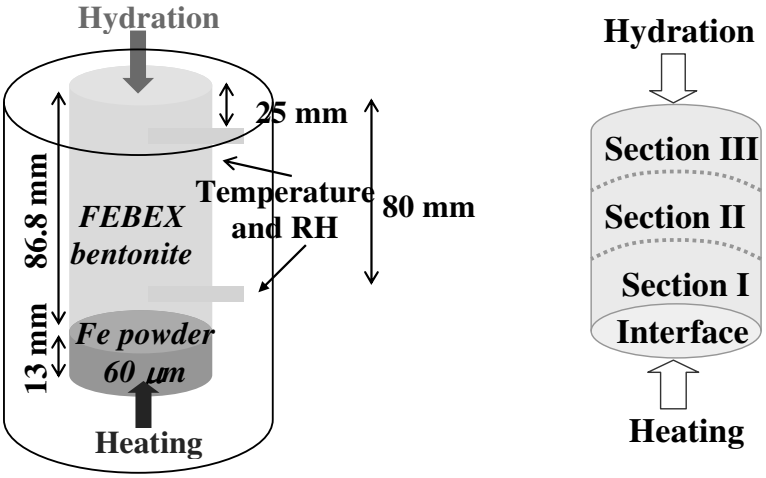

Figure 1. *a) Scheme of the cylindrical cells used; b) Sampling of the bentonite block.*

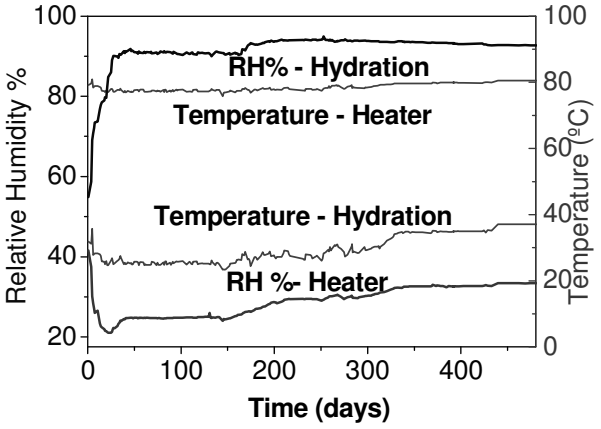

Figure 2. Evolution of Relative Humidity and Temperature recorded by the sensors installed at 0.7 (heater) and 6.2 (hydration) cm from the Fe/bentonite interface.

Geochemical characterization

The hydration of bentonite leads to the dissolution of the soluble accessory minerals in the bentonite (sulfates, carbonates and chlorides). The anions can have a significant influence on corrosion processes. Carbonates can precipitate at the interface as siderite ($FeCO_3$), once the

barrier is fully saturated. Chlorides and sulfates are hygroscopic salts and their precipitation can favour initiation or enhancement of corrosion processes, even at low RH. As expected, soluble carbonates were only detected in saturated areas (934 and 980 mg of CO_3^{2-} per kilogram of dry bentonite, for the cell dismantled after 6 and 15 months, respectively). Figure 3 shows the advance of the chloride and sulfate fronts towards the heater. In the cell dismantled after 15 months, it is observed that most of soluble chloride is concentrated at the interface. So, it seems that after the initial precipitation of chlorides when heating started, there was a later precipitation that resulted from the advective transport of chloride towards the heater. Sulfate concentration is controlled by gypsum solubility. So, in both tests, the sulfate concentration at the interface is much smaller than that of chloride.

Soluble cations, measured in the aqueous extracts, increased as well with time in all the sections, especially in section I and at the Fe/bentonite interface. Cations move much more slowly than anions. Sodium is the main counterion (figure 4). Ca increases with longer times due to dissolution of calcite in the hydrated zones.

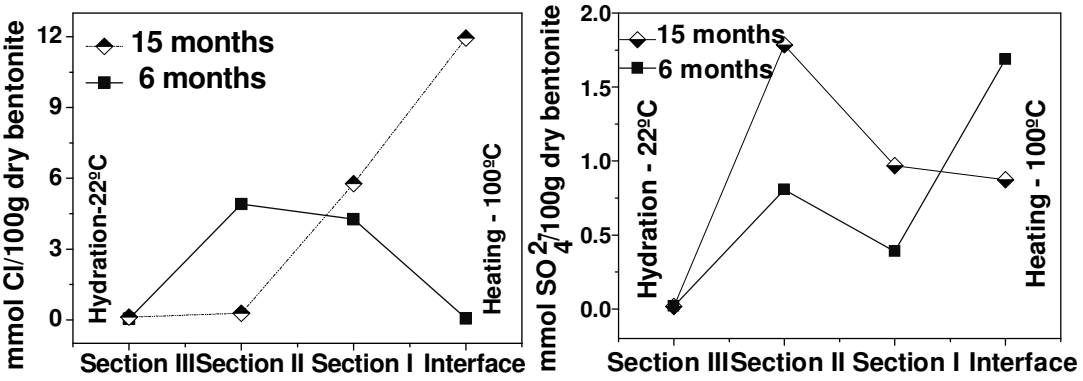

Figure 3. Movement of chlorides (left) and sulfates (right) along the bentonite block (aqueous extract solid:liquid 1:8).

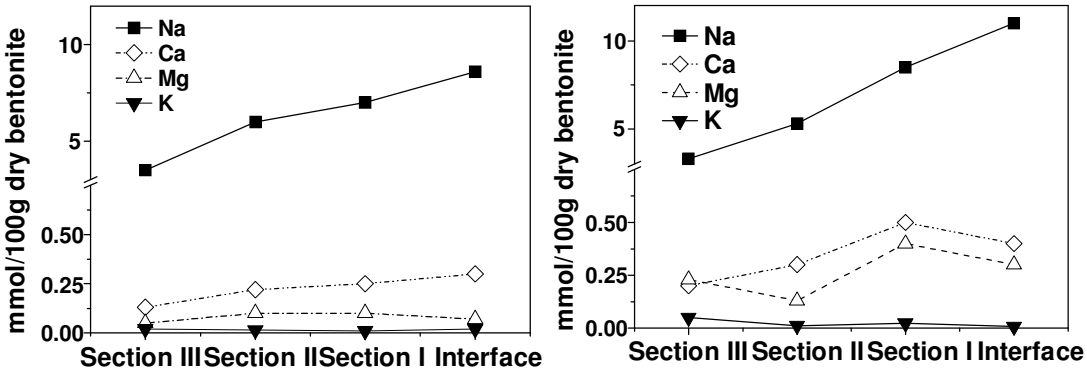

Figure 4. Na, Mg, Ca and K measured in the aqueous extracts: (left) 6-month, (right) 15-month test.

The distribution of the exchangeable cations is modified by the thermal gradient (figure 5). Na seems to substitute Mg in saturated areas (sections III and II), whereas near the Fe/bentonite interface, Na is replaced by Mg in the exchange complex (section I). Magnesium

complexes are thought to be more stable at high temperature than Na, Ca or K-complexes [4]. This fact would be in good agreement with the experimental data obtained in both experiments.

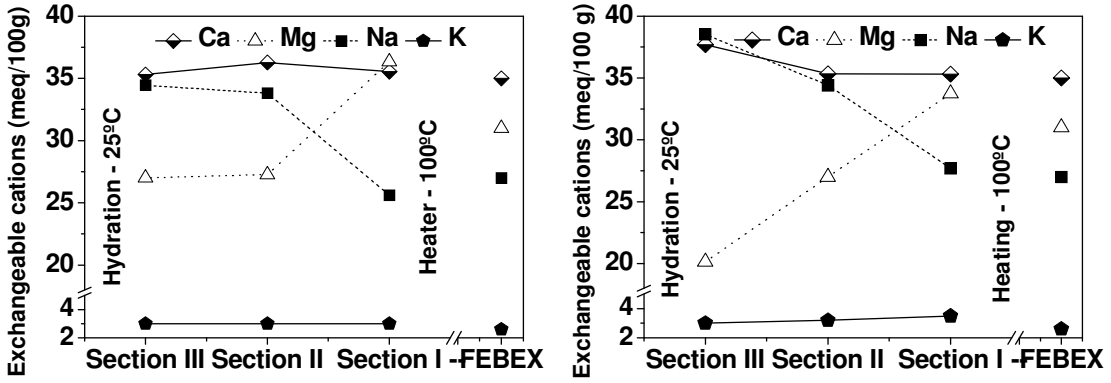

Figure 5. Distribution of exchangeable cations along the bentonite block: (left) 6 months (right) 15 months.

Corrosion products

Different corrosion products were found in the Fe powder depending on the distance from the interface. Oxides were found in both experiments at the interface (figure 6). In the case of the cell dismantled after 6 months, room temperature Mössbauer spectra of the bentonite collected at the interface shows a sextet (quadrupolar splitting: -0.27 mm/s; isomeric shift: 0.25 mm/s; hyperfine field: 100-350 KOe) typical of goethite. In the FTIR spectra recorded for the Fe oxide found at the interface after 15 months, there is a doublet placed at 570 and 478 cm^{-1}. These bands are characteristic of hematite. EDS analysis detected high contents of chlorine (up to 5% at. in some cases), and traces of common elements present in bentonite either in goethite or in hematite.

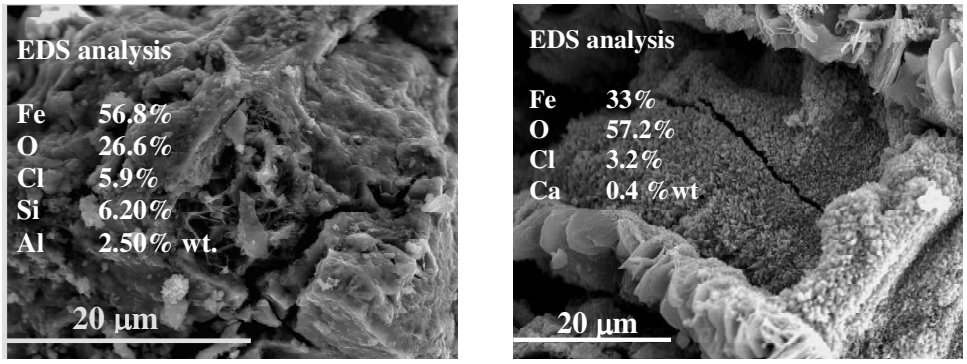

Figure 6. SEM images of Fe oxides found at the Fe/bentonite interface: (Left) goethite in the six-month test; (Right) hematite formed after 15 months of experiment. (EDS analysis was performed over the whole image).

Iron powder that was not in direct contact with bentonite seemed to undergo slight corrosion. In the cell dismantled after 6 months, iron powder away from the bentonite interface kept its metallic luster and no corrosion products could be identified in it. In the cell dismantled after 15 months, corroded and non-corroded areas were observed throughout the iron powder. EDS analysis of corroded Fe powder detected, in most cases, traces of chlorine (0.6% at.) and Ca

(0.3% at.). Precipitation of chloride was not homogeneous and where it was found, a thin layer of hematite (α-Fe_2O_3) (figure 7 left) and maghemite (γ-Fe_2O_3), was grown (below 1 μm in all cases). At this stage, corrosion may continue, however to a lesser extent, as RH at the interface is below 50%. Although the chloride content measured at the interface in the 15-month test is very high, close to 7% wt. (figure 7 right), no Cl-containing phases have been identified.

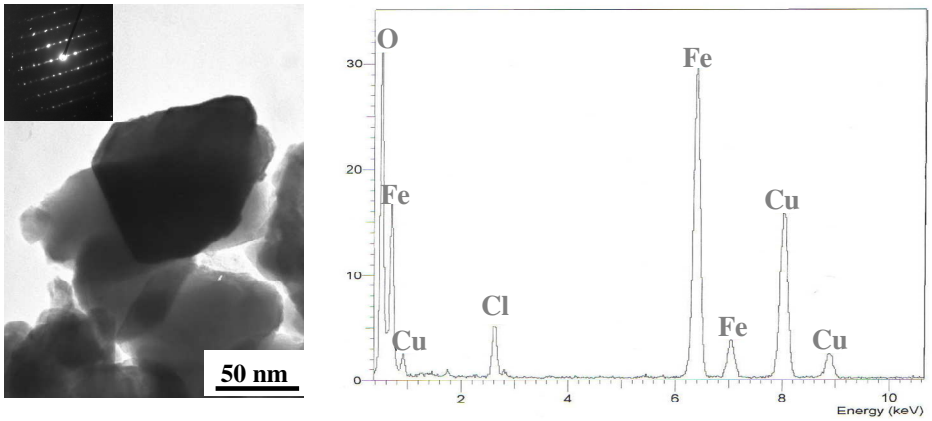

Figure 7. (Left) TEM image of a hematite suspension obtained from corroded Fe powder and SAED pattern of one of the crystals; (right) EDS analysis of the diffracted crystal (Cu lines corresponds to the copper grid in which the hematite suspension was deposited for TEM observation).

CONCLUSIONS

Initial precipitation of chloride plays a relevant role in the first stages of the corrosion process, as it helps to initiate the nucleation of goethite. When bentonite at the interface gets desiccated, goethite can transform into hematite. Once the chloride front reaches the interface and precipitates onto the Fe powder, it seems that corrosion is enhanced again. Results obtained in these tests are preliminary and will be completed after the dismantling of the four experiments on-going at the moment.

ACKNOWLEDGEMENTS

This is a contribution to the NF-Pro project IP number FIGW- CT-2003-02389 financed by the EU and the CIEMAT/ENRESA association.

REFERENCES

1. V. Kucera and E. Mattson, Atmospheric Corrosion in *Corrosion Mechanisms*, edited by F. Mansfeld (Marcel Dekker, Inc., New York, 1987), p.211-252.
2. J. C. Estill and G.E. Gdowski, in *Proceedings of the Seventh International Conference on High Level Radioactive Waste Management*, edited by Holly A. Dockery, (ASCE, New York, 1996), pp. 457-458.
3. B.L. Shawney, Clays and Clay Miner, 18, 47 (1970).
4. J. Cuevas, M.V. Villar, A.M. Fernández, P. Gómez and P.L. Martín, Appl. Geochem, 12, 473 (1997).